Electronic Supplementary Material (ESI) for Journal of Materials Chemistry B.

SUPPORTING MATERIAL

NUIG4: A Biocompatible pcu Metal-Organic Framework with an Exceptional Doxorubicin Encapsulation Capacity

Ahmed Ahmed,[a,b] Constantinos G. Efthymiou,[b,c] Rana Sanii,[a,d] Ewa Patyk-Kazmierczak,[e] Amir M. Alsharabasy,[f] Meghan Winterlich,[b,f] Naveen Kumar,[a,d] Debobroto Sensharma,[a,d] Wenming Tong,[g] Sarah Guerin,[a,h] Pau Farras,[g] Sarah Hudson,[a,d] Damien Thompson,[a,h] Michael J. Zaworotko,*[a,d] Anastasios J. Tasiopoulos,*[c] and Constantina Papatriantafyllopoulou *[a,b,f]

[a.] *SSPC the Science Foundation Ireland Research Centre for Pharmaceuticals*

[b.] *School of Chemistry, College of Science and Engineering, National University of Ireland Galway, H91 TK 33 Galway, Ireland; E-mail address: constantina.papatriantafyllopo@nuigalway.ie; Tel: +353 91 493462.*

[c.] *Department of Chemistry, University of Cyprus, 1678 Nicosia, Cyprus.*

[d.] *Department of Chemical Sciences, Bernal Institute, University of Limerick, Limerick, V94T9PX, Republic of Ireland.*

[e.] *Faculty of Chemistry, Adam Mickiewicz University in Poznań, Uniwersytetu Poznanskiego 8, Poznan, Poland.*

[f.] *CÚRAM, SFI Research Centre for Medical Devices, National University of Ireland Galway, Ireland.*

[g.] *School of Chemistry, Energy Research Centre, Ryan Institute, National University of Ireland, Galway (NUI Galway), University Road, H91 CF50 Galway, Ireland.*

[h.] *Department of Physics, Bernal Institute, University of Limerick, Limerick, Republic of Ireland.*

Experimental

Synthesis of 4-((4-carboxybenzylidene)amino)benzoic acid ($CBABH_2$)

4-Formylbenzoic acid, 4-CHO(Ph)CO_2H (1.00 g, 6.66 mmol) and 4-aminobenzoic acid, 4-NH_2(Ph)CO_2H (0.92 g, 6.66 mmol) were dissolved in EtOH (30 ml) giving a pale yellow solution. The solution was stirred at room temperature for 2 hours after which time a white precipitate was formed. The precipitate was collected by vacuum filtration, washed with EtOH and dried *in vacuo* at 60°C for 24 hours. Yield: 90% ^{1}H-NMR: (400 MHz, DMSO-d6) δ 8.74 (s, 1H), 8.08 (d, 4H), 8.00 (m, 2H), 7.36 (m, 2H) ^{13}C-NMR: (400 MHz, DMSO-d6) δ 167.0, 161.7, 155.0, 139.1, 130.7, 129.8, 129.0, 128.7, 121.2. FTIR cm^{-1} 3333(b), 1692(s), 1592(w), 1548(s), 1376(s). The preparation of the ligand was based on a previously reported synthetic process.[1]

Physical Studies

IR spectra (4000– 400 cm^{-1}) were recorded using a Perkin Elmer 16PC FT-IR spectrometer with samples prepared as KBr pellets. PXRD data were collected using an Inex Equinox 6000 diffractometer at room temperature and pressure. TGA experiments were performed on a STA625 thermal analyser from Rheometric Scientific (Piscataway, New Jersey). The heating rate was kept constant at 10 °C/min, and all runs were carried out between 20 and 600 °C. The measurements were made in open aluminium crucibles, nitrogen was purged in ambient mode, and calibration was performed using an indium standard. Solid-state UV studies were carried out using an Agilent Cary 5000 UV-Vis-NIR spectrophotometer. Fluorimetry studies were carried out on an Agilent Cary Eclipse fluorescence spectrophotometer.

Carbon-13 solid-state nuclear magnetic resonance (ssNMR) spectra were acquired on a Bruker Avance III HD NMR spectrometer operating at B_0 = 9.4 T, with corresponding 1 H and ^{13}C resonance frequencies of $\nu_0(^1H)$ = 400.1 MHz and $\nu_0(^{13}C)$ = 100.6 MHz. **NUIG4**, DOX and DOX@**NUIG4** solid forms were packed in 4 mm o.d. zirconia rotors with Kel-F caps under ambient atmosphere, and experimental ^{13}C NMR spectra were acquired at natural abundance using a 4 mm triple channel (H/X/Y) Bruker MAS probe operating in double resonance mode. The magic angle was optimized using a rotor packed with KBr and spun at 5 kHz. NMR spectra were referenced to TMS at δiso = 0 ppm by setting the high frequency 13C resonance in adamantane to 38.48 ppm.[2] The ^{13}C CPMAS NMR spectra were acquired in a single spectral window using the cross-polarization pulse sequence, with a magic-angle spinning (MAS) rotor frequency of 10 kHz, a ^{1}H 90° pulse width of 2.5 µs, and 50 kHz 1 H decoupling during acquisition. Proton decoupling was carried out with the SPINAL6466 decoupling sequence at 100%. For each sample, the ^{1}H T_1 relaxation time(s) were checked using the saturation recovery pulse sequence to ensure that the

recycle delay allowed for adequate relaxation between the collection of subsequent transients. ^{13}C CPMAS spectra were collected using optimised contact times and relaxation delays (at least 1.4 × T_1 values) for each sample. The optimised parameters DOX were a contact time of 2.5 ms, relaxation delay of 2 s, and 500 scans; for DOX@**NUIG4**, contact time was 2.5 ms, relaxation delay 3 s, and 500 scans; for **NUIG4**, contact time was 4 ms, relaxation delay 3 s, and 500 scans.

Gas Sorption Measurements

For gas sorption experiments, ultrahigh-purity gases were used as received from BOC Gases Ireland: research-grade He (99.999%), CO_2 (99.995%), C_2H_2 (98.5%), C_2H_4 (99.92%), C_2H_6 (99%), N_2 (99.998%) and CH_4 (99.995%). Adsorption experiments (up to 1 bar) for 77 K N_2 and 195 K CO_2 were performed on Micromeritics Tristar II 3030. Micromeritics 3Flex surface area and pore size analyser 3500 was used for collecting 298 K sorption isotherms for C_2H_2, C_2H_4, C_2H_6 and CO_2. Before sorption measurements, activation of **NUIG4** was achieved by degassing the air-dried sample on a SmartVacPrep™ using dynamic vacuum and heating for 16 h (from RT to 333 K with a ramp rate of 5 °C). The Brunauer-Emmett-Teller (BET) surface area of **NUIG4** was determined from the N_2 adsorption isotherm at 77 K (Table S1) as per the criteria set out by Roquerol *et al*.[3] About 100 mg of **NUIG4** sample was used for all the sorption measurements. The bath temperatures of 273 and 298 K were controlled with a Julabo ME (v.2) recirculating control system containing a mixture of ethylene glycol and water. The low temperatures at 77 K and 195 K were maintained by a 4 L Dewar filled with liquid N_2 and a dry ice-acetone mixture, respectively.
Samples were regenerated after each isotherm by degassing over 3 h.

IAST selectivities for selected adsorbate mixtures were calculated from pure-component adsorption isotherms. Single-component adsorption isotherms for each gas at 298 K were fitted to the dual-site Langmuir equation (Equation 1).

$$n(P) = \frac{q_1(k_1P)}{1 + (k_1P)} + \frac{q_2(k_2P)}{1 + (k_2P)} \quad (1)$$

Once the isotherms were parametrised, mixed-gas fractional uptakes were determined, and finally the selectivity, $S_{i/j}$, was obtained using Equation 2. Here, x_i and x_j are the mole fractions of components *i* and *j*, respectively, in the adsorbed phase, and y_i and y_j are the mole fractions of components *i* and *j* in the gas phase respectively.

$$S_{i/j} = \frac{(x_i/x_j)}{(y_i/y_j)} \quad (2)$$

Dual-site Langmuir parameters for various equations are listed in Table S2.

Table S1. BET fitting parameters from 77 K N_2 and 195 K CO_2 isotherms for **NUIG4**.

Adsorbate	N_2 77 K	CO_2 195 K
BET surface area	1,358.3026 ± 1.0507 m²/g	1,229.3448 ± 37.6530 m²/g
Slope	0.003204 ± 0.000002 g/cm³ STP	0.003647 ± 0.000114 g/cm³ STP
Y-intercept	0.000001 ± 0.000000 g/cm³ STP	0.000069 ± 0.000004 g/cm³ STP
C	5,368.771124	53.928369
Q_m	312.0685 cm³/g STP	269.1493 cm³/g STP
Correlation coefficient	0.9999991	0.9923069
Molecular cross-sectional area:	0.1620 nm²	0.1700 nm²

Table S2. IAST fitting parameters to the Dual-Site Langmuir equation for various gases on **NUIG4** at 298 K.

Adsorbate	R^2 value	q_1 (mmol g^{-1})	k_1 (bar^{-1})	q_2 (mmol g^{-1})	k_2 (bar^{-1})
CO_2	0.999999	1.4444	1.52833	33.568	0.0361713
C_2H_2	0.999984	0.427405	11.1437	11.0621	0.450622
C_2H_4	0.999996	0.323944	6.86233	5.45936	0.962384
C_2H_6	0.999997	0.072033	21.4207	5.2187	2.18709

X-ray Crystallography

Crystallographic data for **NUIG4** were collected at room temperature on a Bruker D8 Quest fixed-Chi single crystal diffractometer, equipped in Photon II detector and IμS micro-focus Cu anode (λ=1.54178 Å). Program APEX3 was used for data collection, while programs SAINT V8.38A and SADABS-2016/2 (implemented in APEX3), were used for data reduction and absortion correction, respectively.[4] The structure was solved with intrisinc phasing using ShelXT, and refined with least squares method with ShelXL, both implemented in Olex2 program.[5] The non-H atoms were treated anisotropically, whereas the hydrogen atoms were placed in calculated, ideal positions and refined as riding on their respective carbon atoms. Due to the poor diffracting properties of the crystal, limiting the resolution and quality of the collected data, restraints and constraints were used for the structural model, and the electron density associated with the content of the pores was excluded from the refinement by using solvent mask

implemented in Olex2.[6] The measured crystal was an inversion twin (BASF=0.3) containing domains of different chirality with symmetries $P4_1$ and $P4_3$ in a 7:3 ratio.

The crystal structure has been deposited with the Cambridge Crystallographic Data Centre (CCDC 2109469),[7] and can be accessed, free of charge, by filling the application form at https://www.ccdc.cam.ac.uk/structures/. The most important structural data and refinement details are listed in Table S3 in Supporting Information.

Table S3. Crystallographic data for **NUIG4.**

	NUIG4
Formula	$C_{45}H_{27}N_3O_{13}Zn_4$
Mw	1079.17
Crystal System	Tetragonal
Space group	$P4_1$
a/ Å	19.146(2)
c/ Å	19.117(2)
V/ Å ^{3}	7008(2)
Z	4
T/ K	301(2)
λ/ Å	1.54178
D_c/g cm^{-3}	1.023
μ(Mo Ka)/mm^{-1}	1.923
Reflections collected	14854
Independent reflections	4024
Flack parameter	0.30(16)
R_1[a], wR_2[b] [I > 2σ(I)]	0.0955, 0.2472
R_1[a], wR_2[b] (all data)	0.1188, 0.2714
Goodness of fit on F^2	1.037
Δρmax/ $\Delta\rho_{min}$ /e Å $^{-3}$	0.579 /-0.664

[a] $R_1 = \Sigma(||F_o| - |F_c||)/\Sigma|F_o|$; [b] $wR_2 = [\Sigma[w(Fo^2 - Fc^2)^2]/\Sigma[wFo^2)^2]]^{1/2}$

DOX adsorption and release studies

DOX (0.04 g) was dissolved in MeOH:DMSO (9:1, 10 ml) and added to a centrifuge vial that contained **NUIG4** (0.01 g). At specified time intervals the supernatant was centrifuged and 25 μL aliquots of the solution were removed and dissolved in MeOH (5 ml). The uptake of the drug was then monitored by UV-Vis spectroscopy and HPLC. For the release studies, loaded **NUIG4** (50 mg) was suspended in distilled H_2O or PBS/5.5 pH sodium acetate buffer solution (10 ml) and stirred at 37°C. At specified time intervals the solution was centrifuged and 100 μL aliquots of the solution were removed and diluted in distilled H_2O or PBS solution (5 ml) and 100 μL of fresh solution was added into the vial. The release of DOX was then monitored by UV-Vis spectroscopy and HPLC.

In vitro Studies

MDA-MB-231 cells (HTB-26™) and Normal Adult Human Primary Dermal Fibroblasts (HDFs, PCS-201-012™), obtained from the American Type Culture Collection, were used to evaluate the cytocompatibility of the of the organic linker $CBABH_2$, **NUIG4**, DOX and DOX@**NUIG4**. The HDFs were cultured in Dulbecco's modified Eagle's medium (DMEM, Invitrogen), containing 1% penicillin/streptomycin and 10% (v/v) fetal bovine serum (FBS, Sigma-Aldrich), while MDA-MB-231 were maintained in in RPMI-1640 medium (Sigma-Aldrich) supplemented with 2 mM L-glutamine (Sigma-Aldrich) and 10% FBS. The cells were harvested using 0.25% of trypsin-EDTA (Sigma-Aldrich), seeded at a density of 15,000 and 5000 cells/well in the case of MDA-MB-231 and HDFs, respectively. and allowed to grow in a humidified atmosphere of 5% CO_2 and 20% O_2 for 24 h at 37 °C. Stock solutions of $CBABH_2$, **NUIG4**, DOX and DOX@**NUIG4** were prepared in DMSO, vortexed, sterile filtered, and the cells were then treated with different concentrations of each one diluted in FBS-free medium. The cells were cultured for 72 hrs and both the metabolic activity and cell viability were measured each day. In brief, the culture media were discarded, and each well was washed with PBS, and for metabolic activity assessment, 150 µL of fresh Quant™ AlamarBlue Cell Viability Reagent (Thermo Fisher Scientific) (10%) were added and the cells were incubated in 5% CO_2 for 3 h at 37◦C. This was followed by measuring the fluorescence of solution at an excitation of 550 nm and emission of 590 nm on a VarioskanFlash-4.00.53 microplate reader (Thermo Fisher Scientific, Finland). The metabolic activity under each treatment was calculated by normalizing the fluorescence reading to that one of the untreated cells. The viability of cells was evaluated using live/dead viability assay, where 100 µL of PBS solution containing 1 µM calcein AM (Invitrogen) and 2 µM Ethidium homodimer (EthD-1, Sigma-Aldrich) were added to each washed well, and the cells were incubated for 20 min at 37 °C. The cells were then imaged using the Operetta high-content imaging system (PerkinElmer, Waltham, MA), where calcein AM was excited at 494 nm and detected using the filter for Alexa Fluor™ 488, while the filter for propidium iodide was employed for detection of cells stained by EthD-1. Three samples were tested per each evaluated concentration from each group at each time-point. All data were statistically compared with one-way analysis of variance (ANOVA) tests.

Molecular Modelling

All calculations were carried out using the Vienna Ab initio Simulation Package (VASP),[8] with plane wave basis sets[9] and the projector augmented-wave (PAW) method.[10] Exchange-correlation effects were treated using density functional theory[11] (DFT) *via* the Perdew, Burke, and Ernzerhof (PBE) implementation[12] of the Generalised Gradient Approximation[13] (GGA) with Grimme D3 dispersion corrections.[14] Single Γ-centred k-point relaxations (using

conjugate gradient minimization[15]) were carried out using a plane wave cut-off of 800 eV and Gaussian smearing with smearing width of 0.05 eV. Projection operators were evaluated in real-space with automatic optimization. The CBAB ligand was extracted from the optimized crystal structure, and the DOX structure was downloaded from the protein data bank (PDB, ligand DM2). Molecules were placed within binding distance of each other and possible binding configurations sampled at rotations of 30° and allowed to relax into the most favourable binding orientations (based on the lowest ground state energy, similar to previous binding energy studies[16, 17]). Each complex was pre-optimised using Avogadro[18], and then fully optimised in VASP using the methhodology above. Once the most favourable molecular orientations were found, binding energies (E_b) were calculated as the total ground state energy of the complex minus the sum of ground state energies of each of the isolated DOX and $CBABH_2$. The binding energy is then: $E_b = E_{DOX:CBAB} - E_{DOX} - E_{CBAB}$

Table S4. Selected interatomic distances (Å) and angles (°) for **NUIG4**.

Bonds			
Zn1-O1W	1.917(13)	Zn3-O1W	2.072(16)
Zn1-O3B	2.035(11)	Zn3-O3C	2.204(9)
Zn1-O19A	1.830(14)	Zn3-O20A	1.942(16)
Zn1-O20C	2.044(11)	Zn3-O20B	1.914(13)
Zn2-O1B	2.111(11)	Zn4-O1A	1.997(14)
Zn2-O1C	1.978(10)	Zn4-O1W	1.864(16)
Zn2-O1W	1.916(13)	Zn4-O19B	1.889(15)
Zn2-O3A	1.910(15)	Zn4-O19C	2.041(12)
Angles			
O3B-Zn1-O20C	93.8(2)	O20B-Zn3-O1W	93.9(6)
O19A-Zn1-O1W	119.8(5)	O20B-Zn3-O3C	142.8(3)
O3A-Zn2-O1B	98.7(4)	O1A-Zn4-O19C	99.1(3)
O1W-Zn2-O1C	115.9(5)	O1W-Zn4-O19B	120.9(6)

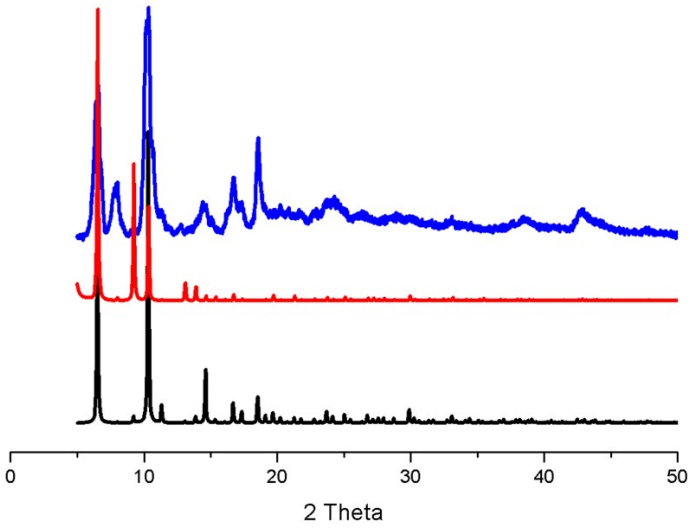

Figure S1. PXRD patterns of the **NUIG4** as synthesized (red) and activated (blue) in comparison to the theoretical one (black).

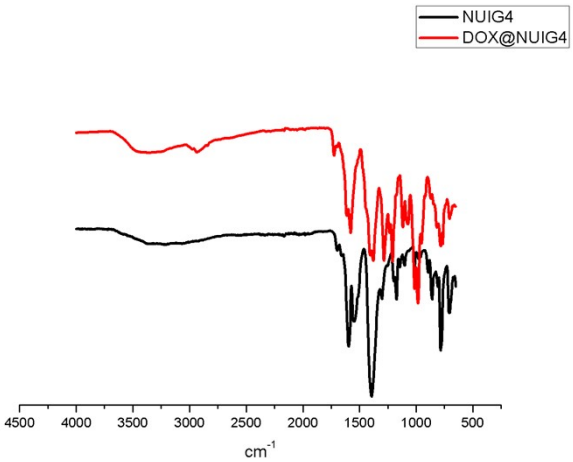

Figure S2. FTIR spectra of **NUIG4** and DOX@**NUIG4**.

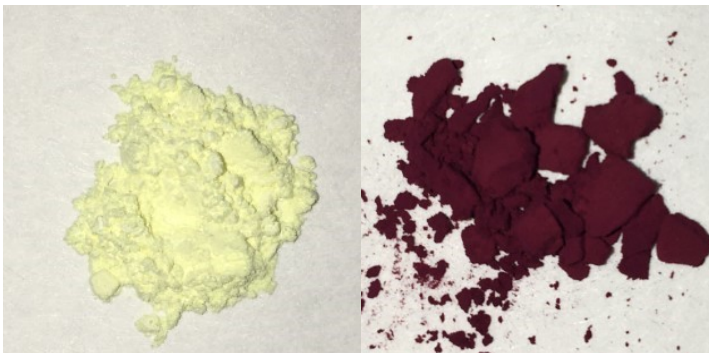

Figure S3. Photographs showing the colour change of **NUIG4** (left) upon DOX encapsulation (right).

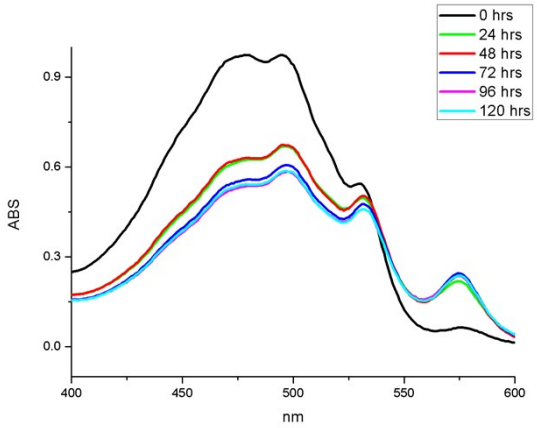

Figure S4. UV-Vis data for DOX uptake by **NUIG4**.

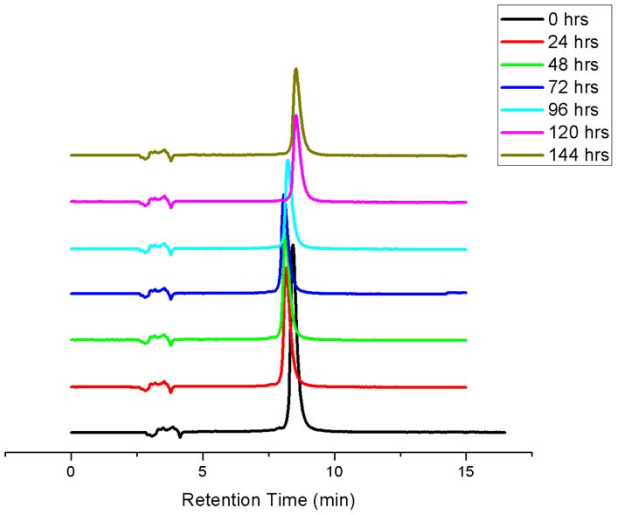

Figure S5. HPLC data showing the uptake of DOX after 144 hours.

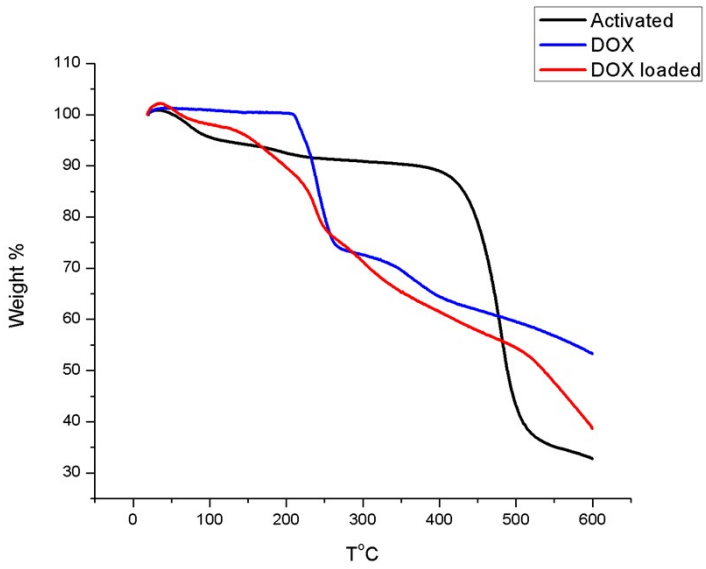

Figure S6. Thermogravimetric analysis plots for **NUIG4**, DOX and DOX@**NUIG4**.

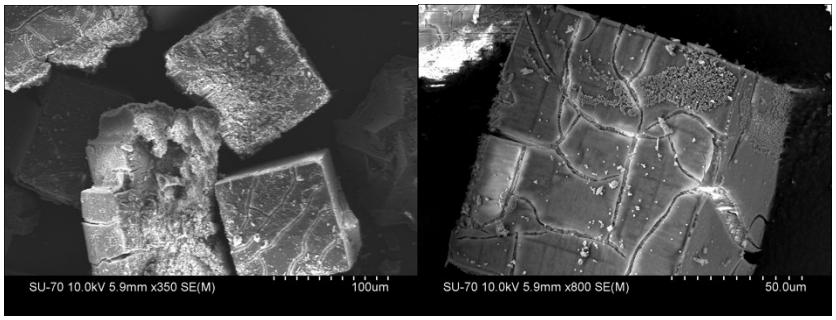

Figure S7. SEM images of DOX@**NUIG4**.

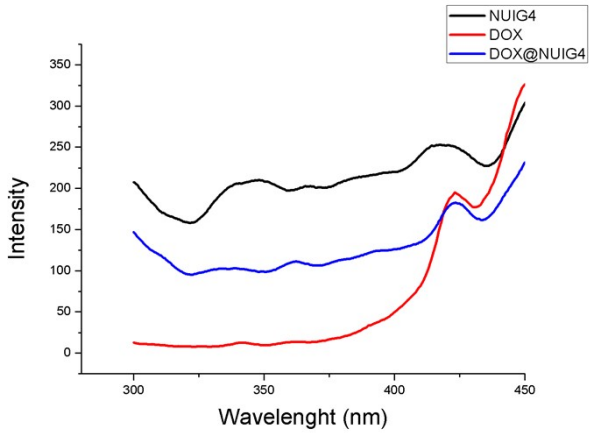

Figure S8. Fluorescence emission spectra upon excitation at 250 nm.

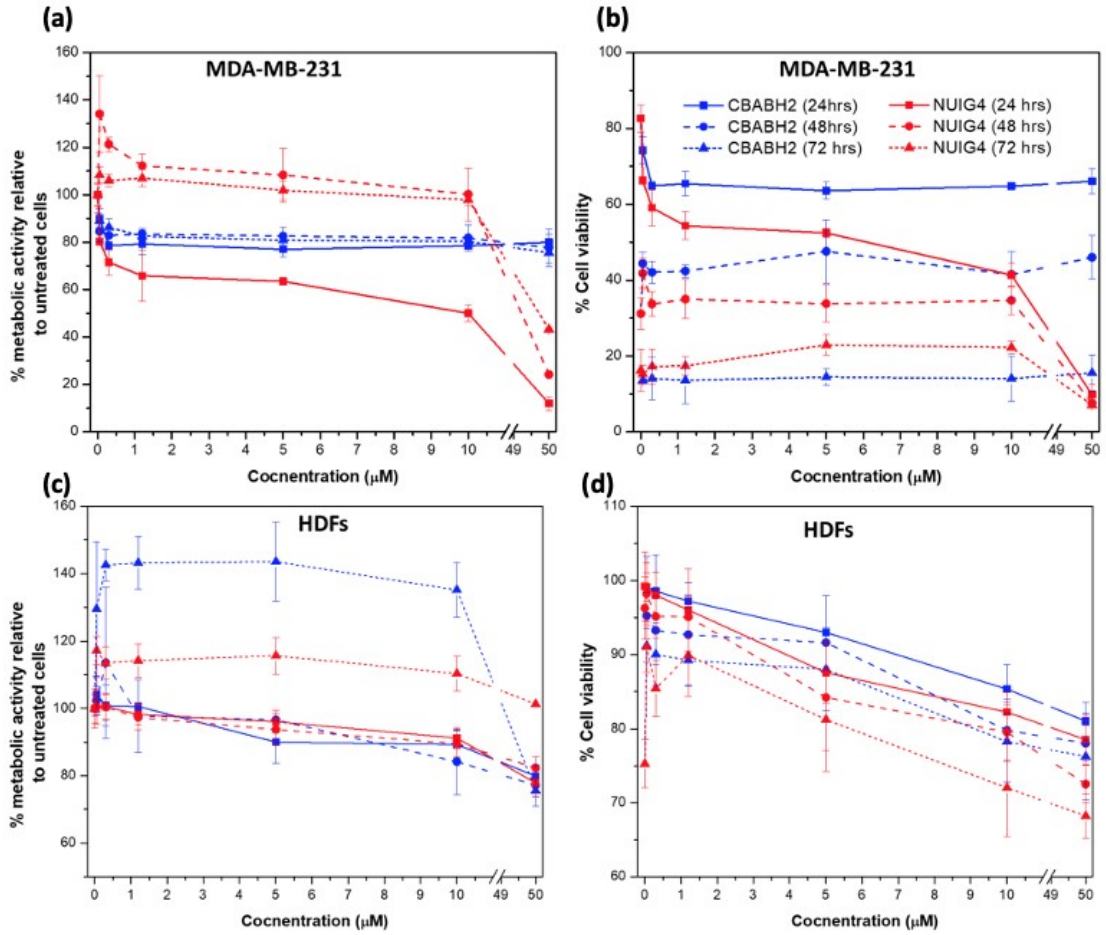

Figure S9. Effects of the organic linker $CBABH_2$ and **NUIG4** treatment on the metabolic activity **(a** and **c)** and viability **(b** and **d)** of HDFs and MDA-MB-231 cells. Both cell lines were treated with different concentrations of $CBABH_2$ and **NUIG4** within the range of 0.3- 50 µM for 72 h as described in the methods. The metabolic activity, measured by AlamarBlue assay and viability of cells, measured by calcein AM/ EthD-1 live/dead staining, were investigated after 24 **(solid line)**, 48 **(dashed line)** and 72 **(short dashed line)** hours of culture. **blue colour:** CBABH2; **Red colour: NUIG4**. The data represent the mean ± SD (standard deviation) of three samples.

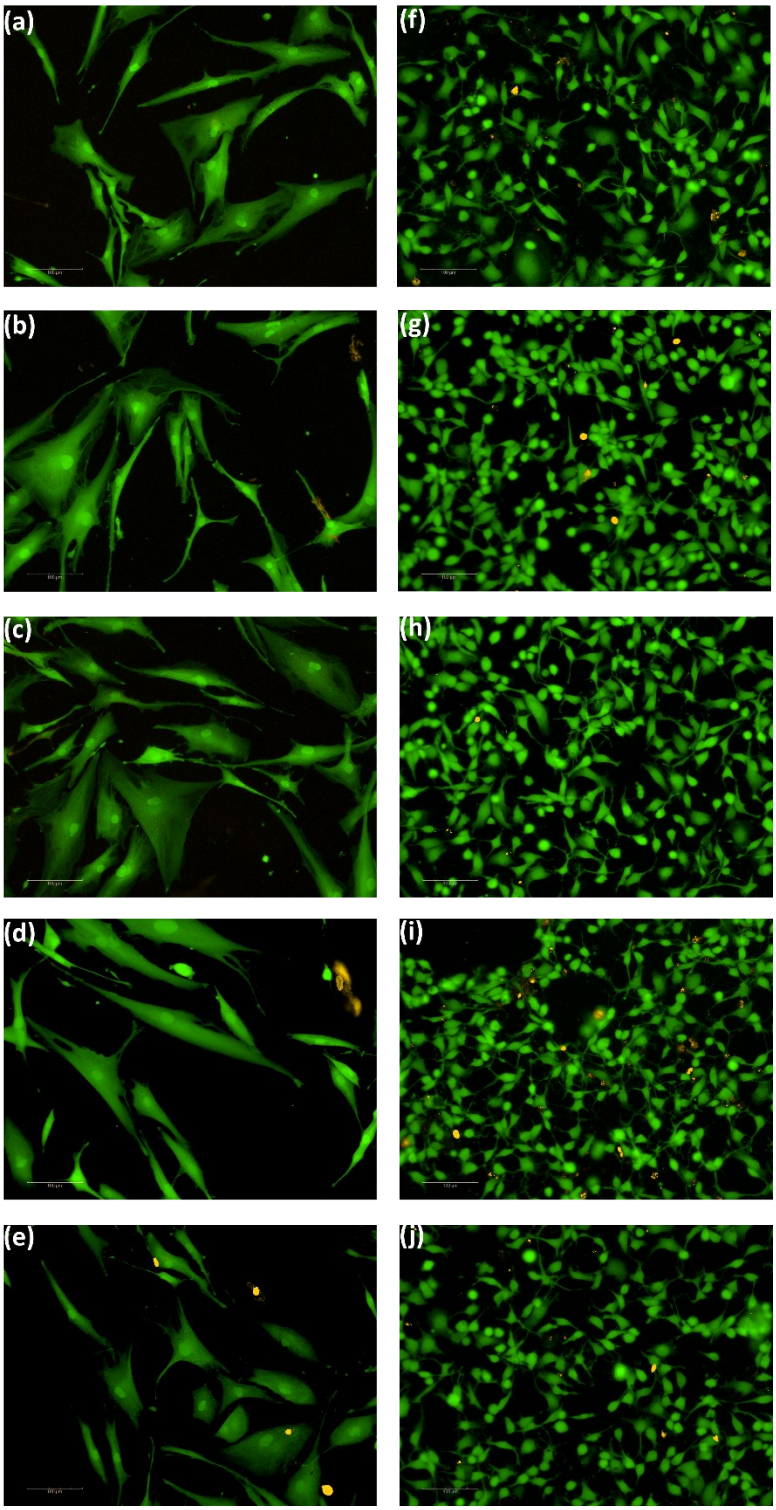

Figure S10. Calcein-AM and EthD -1 live/dead staining of HDFs **(a-e)** and MDA-MB-231 **(f-j)**. The representative photos are for cells, which were cultured in either FBS-free medium only **(a, f)** or treated with 1.2 µM $CBABH_2$ **(b, g), NUIG4 (c, h),** DOX **(d, i)**, or DOX@**NUIG4 (e, j)** for 24 hrs**.** Scale bar: 100 µm.

References

1 S. Yuan, L. F. Zou, H. X. Li, Y. P. Chen, J. S. Qin, Q. Zhang, W. G. Lu, M. B. Hall and H. C. Zhou, *Angew. Chem. Int. Ed*., 2016, **55**, 10776.
2 C. R. Morcombe and K. W. Zilm, *J. Magn. Reson*. 2003, **162**, 479.
3 M. Thommes, K. Kaneko, A. V. Neimark, J. P. Olivier, F. Rodriguez-Reinoso, J. Rouquerol and K. S.W. Sing, *Pure Appl. Chem*., 2015, **87(9-10)**, 1051.
4 a) APEX3, Ver. 2017.3-0. Bruker AXS Inc., Madison, Wisconsin, USA, 2017; b) SAINT, Ver. 8.38A. Bruker AXS Inc., Madison, Wisconsin, USA, 2016; c) SADABS, Ver 2016/2. Bruker AXS Inc., Madison, Wisconsin, USA, 2016.
5 a) G. M. Sheldrick, *Acta Crystallogr. Sect. Found. Adv.* 2015, **71(1)**, 3; b) G. M. Sheldrick, *Acta Crystallogr. Sect. C Struct. Chem.* 2015, **71(1)**, 3; c) O. V. Dolomanov, L. J. Bourhis, R. J.Gildea, J. A. K. Howard and H.Puschmann, *J. Appl. Cryst*. 2009, **42**, 339.
6 P. van der Sluis and A. L. Spek, *Acta Cryst*. 1990, **A46**, 194.
7 C. R. Groom, I. J. Bruno, M. P. Lightfoot and S. C. Ward, *Acta Crystallogr. Sect. B Struct. Sci. Cryst. Eng. Mater.* 2016, **72(2)**, 171.
8 J. Hafner, *J. Comput. Chem*., 2008, **29**, 2044.
9 G. Kresse and J. Furthmüller, *Phys. Rev. B*, 1996, **54**, 11169.
10 G. Kresse and J. Furthmüller, *Phys. Rev. B*, 1999, **59**, 1758.
11 C. Fiolhais, F. Nogueira and M. A. Marques, Springer Science & Business Media: 2003; Vol. 620.
12 J. P. Perdew and W. Yue, *Phys. Rev. B*, 1986, **33**, 8800.
13 J. P. Perdew, K. Burke and M. Ernzerhof, *Phys. Rev. Lett*., 1996, **77**, 3865.
14 S. Grimme, J. Antony, S. Ehrlich, and H. Krieg, *J. Chem. Phys*, 2010, **132**, 154104.
15 I. Štich, R. Car, M. Parrinello and S. Baroni, *Phys. Rev. B*, 1989, **39**, 4997.
16 P. Song, S. Guerin, S. J. R. Tan, H. V. Annadata, X. Yu, M. Scully, Y. M. Han, M. Roemer, K. P. Loh, D. Thompson, *Adv. Mat*., 2018, **30**, 1706322.
17 R. Shaikh, S. Shirazian, S. Guerin, E. Sheehan, D. Thompson, G. M. Walker and D. M. Croker, *Int. J. Pharm*., 2021, 120514.
18 M. D. Hanwell, D. E. Curtis, D. C. Lonie, T. Vandermeersch, E. Zurek and G. R. Hutchison, *J. cheminformatics*, 2012, **4**, 17.